1 # Mechanistic numerical modeling of solute uptake by plant roots
2 # A mechanistic solution for the combined water and solute uptake
3 # by plant roots

4 Andre Herman Freire Bezerra * Quirijn de Jong van Lier
5 Sjoerd E.A.T.M van der Zee Peter de Willingen (acknowledgements?)

6 January, 2016

*Bezerra, A.H.F. and Q. de Jong van Lier, Exact Sciences Dep., ESALQ–Univ. of São Paulo, 13418-900 Piracicaba (SP), Brazil; S.E.A.T.M. van der Zee and P. Willingen, Dep. of Environmental Sciences, Wageningen Univ., Droevendaalsesteeg 4, 6708 PB Wageningen, the Netherlands.

Core ideas

- idea 1
- idea 2
- idea 3
- optional idea 4
- optional idea 5

Abstract

A modification in an existing water uptake and solute transport numerical model was implemented in order to allow the model to simulate solute uptake by the roots. The convection-dispersion equation (CDE) was solved numerically, using a complete implicit scheme, considering a transient state for water and solute fluxes and a soil solute concentration dependent boundary for the uptake at the root surface, based on the Michaelis-Menten (MM) equation. Additionally, a linear approximation was developed for the MM equation such that the CDE has a linear and a non-linear solution. A radial geometry was assumed, considering a single root with its surface acting as the uptake boundary and the outer boundary being the half distance between neighboring roots, a function of root density. The proposed solute transport model includes active and passive solute uptake and predicts solute concentration as a function of time and distance from the root surface. It also estimates the relative transpiration of the plant, on its turn directly affecting water and solute uptake and related to water and osmotic stress status of the plant. Performed simulations show that the linear and non-linear solutions result in significantly different solute uptake predictions when the soil solute concentration is below a limiting value (C_{lim}). This reduction in uptake at low concentrations may result in a further reduction in the relative transpiration. The contributions of active and passive uptake vary with parameters related to the ion species, the plant, the atmosphere and the soil hydraulic properties. The model showed a good agreement with an analytical model that uses a linear concentration dependent equation as boundary condition for uptake at the root surface. The advantage of the numerical model is it allows simulation of transient solute and water uptake and, therefore, can be used in a wider range of situations. Simulation with different scenarios and comparison with experimental results are needed to verify model performance and possibly suggest improvements.

Introduction

Plant transpiration is directly affected by responses from abiotic stress like those related to excess or scarcity of water and solute in soil. Modeling arises as a relevant manner of predicting actual transpiration rates based on water and solute movement physical processes, improving predictions of crop growth and productivity. Models of water and solute uptakes are often classified as microscopic, which describe radial flow to single cylindrical roots (Gardner, 1965; Barber, 1974; Cushman, 1979; De Willigen and Van Noordwijk, 1994; Roose et al., 2001; De Jong van Lier et al., 2009), and macroscopic, which describe flow by adding a layered sink term added to the mass balance equations, without considering root geometry (Šimùnek et al., 2006; Somma et al., 1998; Van Dam et al., 2008). Microscopic models have the advantage to implicit simulate water uptake compensation as the uptake is controlled by computed local water potential gradients, whereas macroscopic can simulate processes at greater (plot or field) scales. As of water uptake models, water stress equations also enter in this classification. Macroscopic models for water stress (Feddes et al., 1978; Homaee, 1999; Li et al., 2006) are widely used but they fail when have the disadvantage of being overall empirical, with parameters that does not have a clear physical meaning. Microscopic models better cope with the phenomena as their physical underlying processes are translated in mathematical formulations. De Jong van Lier et al. (2006) proposed a microscopic root water uptake model that predicts the onset of the falling transpiration rate phase, according to a pressure head threshold value (h_{lim}) which is determined by the potential matric flux (M), function of potential transpiration and root length density. (SHOW EQUATION?) cite quirijn 2006 and everton 2016 Their approach brought a physical meaning and reduced the number of parameters of the uptake reduction function. In a later work, De Jong van Lier et al. (2009) introduced the osmotic component to generate a combined water and osmotic stress model.

Solute mobility in soil is described by the processes of convective transport by water mass flow and movement driven by diffusion due to the concentration gradient caused by solute depletion (or accumulation) in the root surface (Barber, 1962). The earlier analytical solutions for the convection-dispersion equation were formulated considering a steady state condition to the water flow and a solute uptake governed by the solute concentration in the soil solution (Barber, 1974; Cushman, 1979; Nye and Marriott, 1969) or determined by a constant plant demand (De Willigen, 1981). A solution considering a 'pseudo-steady state' for water flow and a solute concentration dependent uptake was later proposed by Roose et al. (2001). The concentration limiting (or supply driven) approach may overestimate the uptake in scenarios where solute supply to the root is not limiting (Barraclough and Leigh, 1984) whilst the constant plant demand (or demand driven) formulation may overestimate the uptake when the soil is very dry or at low solute concentration at the root surface, when the diffusive flow prevails. The more realistic model considers both the supply driven uptake when solute in soil is limiting and the demand driven uptake when solute in soil is abundant. As the model gains complexity analytical solutions becomes unfeasible. Numerical models then plays a important role to compute solutions for complex nonlinear models of water and solute uptake, and can be used to estimate water and solute movement under transient conditions (CITE MODELS).

A nonlinear solute uptake boundary condition that can be used as a boundary condition at root surface and with a concentration dependent solute uptake is the Michaelis-Menten equation (Barber, 1995; Barber and Cushman, 1981; Schröder et al., 2012; Šimunek and Hopmans, 2009). The MM equation is supposed to describe well the solute uptake for both anions (Epstein, 1972; Siddiqi et al., 1990; Wang et al., 1993) and cations (Broadley et al., 2007; Kelly and Barber, 1991; Kochian and Lucas, 1982; Lux et al., 2011; Sadana et al., 2005) in the low concentration range and, adding a linear component to the equation, it can properly estimates the uptake rate also for higher concentrations (Borstlap, 1983; Broadley et al., 2007; Epstein, 1972; Kochian and Lucas, 1982; Vallejo et al., 2005; Wang et al., 1993). Many authors agree that for low concentration in external medium, the uptake is driven by an active plant mechanism, as it occurs contrary the solute gradient between root and soil (Epstein's mechanism I). For the high concentration range, solutes are freely transported from soil to roots by diffusion and occasional convection. This passive transport is known as Epstein's mechanism II (Kochian and Lucas, 1982; Siddiqi et al., 1990). Details on Epstein's mechanisms and its physiological mechanisms, as well as on active and passive uptake, are found in Epstein (1960) and Fried and Shapiro (1961).

The values of MM parameters are strongly dependent on the experimental methods used and vary with plant species, plant age, plant nutritional status, soil temperature and pH (Barber, 1995; Shi et al., 2013). Therefore, they have to be determined for each particular experimental scenario. Some types of experiments to determine the kinetic parameters I_m, K_m and C_{min} include hydroponically-grown plants (Barber, 1995) and the use of radioisotopes to estimate them directly from soil (Nye and Tinker, 1977). The latter is more realistic since there is a large difference between a stirred nutrient solution and the complex and dynamic soil medium. Measuring C_{min} is particularly difficult (Lambers et al., 2008; Seeling and Claassen, 1990) because it occurs at very low concentration levels that may be hard to be accurately measured. Seeling and Claassen (1990) show that C_{min} can be neglected for the cases of high K_m values.

The objective of this thesis is to present a modification of the model of root water uptake and solute transport proposed by De Jong van Lier et al. (2009). This modification allows the model to take into account plant solute uptake. To do so, a numerical mechanistic solution for the equation of convection-dispersion will be developed that considers transient flow of water and solute, as well as root competition. A soil concentration dependent solute uptake function as boundary condition at the root surface was assumed. In this way, the new model allows prediction of active and passive contributions to the solute uptake, which can be used to separate ionic and osmotic stresses by considering solute concentration inside the plant. The proposed model is compared with the original model, with a constant solute uptake numerical model and with an analytical model that uses a steady state condition for water content.

The model here proposed considers a supply driven solute uptake and gives opportunity to add a demand driven uptake when considering solute concentration inside the plant when needed.

MATERIAL AND METHODS

Hydraulic Properties and Soil

Water uptake was analyzed using hydraulic data for three topsoils from the Dutch Staring series (Wösten et al., 2001) as listed in Table 1. The Van Genuchten (1980) equation system was used to describe K–θ–h relations for these soils:

$$\theta(h) = \theta_r + \frac{\theta_s - \theta_r}{[1 + |\alpha h|^n]^{1-(1/n)}} \quad (1)$$

$$K(\theta) = K_s \Theta^{\lambda} [1 - (1 - \Theta^{n/(n-1)})^{(1-(1/n))}]^2 \quad (2)$$

where θ ($m^3\ m^{-3}$) is the water content, K ($m\ s^{-1}$) and K_s ($m\ s^{-1}$) are respectively the hydraulic conductivity and the saturated hydraulic conductivity, h is the pressure head (m), Θ (–) is the effective saturation defined by $\frac{(\theta-\theta_r)}{(\theta_s-\theta_r)}$; θ_s ($m^3\ m^{-3}$) and θ_r ($m^3\ m^{-3}$) are the saturated and residual water contents, respectively; and α (m^{-1}), λ (–) and n (–) are empirical parameters.

Table 1: Soil hydraulic parameters used in simulations

Staring soil ID	**Textural class**	**Reference in this paper**	$\boldsymbol{\theta_r}$	$\boldsymbol{\theta_s}$	$\boldsymbol{\alpha}$	$\boldsymbol{\lambda}$	**n**	$\boldsymbol{K_s}$
			$m^3\ m^{-3}$		m^{-1}	–	–	$m\ d^{-1}$
B3	Loamy sand	Sand	0.02	0.46	1.44	-0.215	1.534	0.1542
B11	Heavy clay	Clay	0.01	0.59	1.95	-5.901	1.109	0.0453
B13	Sandy loam	Loam	0.01	0.42	0.84	-1.497	1.441	0.1298

Model Description

Microscopic root uptake models consider a single cylindrical root of radius r_0 (m) with an extraction zone being represented by a concentric cylinder of radius r_m (m) that bounds the half-distance between roots. The height of both cylinders is z (m) and represents the rooted soil depth. The basic assumptions of this type of model is that the root density does not change with depth and there is no difference in intensity of extraction along the root surface. Water and solute flows are axis-symmetric.

It is common to report root length density R ($m\ m^{-3}$) and r_0. These are related to r_m and root length L (m) by the following equations:

$$r_m = \frac{1}{\sqrt{\pi R}} \quad (3)$$

$$L = \frac{A_p z}{\pi {r_m}^2} \quad (4)$$

where A_p (m^2) is the soil surface area occupied by the plant. For the case that there is no available data from literature, one can obtain the value of L from relatively simple measurements of root and soil characteristics as soil mass (m_s, kg) and density (d_s, $kg\ m^{-3}$), and root average radius ($\overline{r_0}$, m) and R by

$$R = \frac{1}{\pi {r_m}^2}\,. \quad (5)$$

The geometry of the soil-root system considers an uniformly distributed parallel cylindrical root of radius r_0 and length z. To each root, a concentric cylinder of radius r_m and length z can be assigned to represent its extraction volume (Figure 1).

The discretization needed for the numerical solution was performed at the single root scale. As the extraction properties of the root are considered uniform along its length, and assuming no vertical differences in root density and fluxes, the cylinder can be represented by its cross-section, a circle. The area of this circle, representing the extraction region, was subdivided into n circular segments of variable size Δr (m), small near the root and increasing with distance, according to the equation De Jong van Lier et al. (2009):

$$\Delta r = \Delta r_{min} + (\Delta r_{max} - \Delta r_{min}) \left(\frac{r - r_0}{r_m - r_0} \right)^S \quad (6)$$

where the subscripts in Δr indicate the minimum and maximum segment sizes defined by the user, and S gives the rate at which the segment size increases. The parameter r_0 (m) represents the root radius, and r_m (m) is the radius of the root extraction zone, equal to the half-distance between roots, which relates to the root density R ($m\ m^{-3}$) according to Equation 3. This variable size discretization has the advantage to result in smaller segments in regions that need more detail in the calculations (near the root soil interface) due to the greater variation of expected fluxes. Figure 2 shows a schematic representation of the discretization as projected by Equation 6.

A fully implicit numerical treatment was given to the water and solute balance equations **??** and **??**. The Richards equation **??** for one-dimensional axis-symmetric flow can be written as

$$\frac{\partial \theta}{\partial t} = \frac{\partial \theta}{\partial H}\frac{\partial H}{\partial t} = C_w(H)\frac{\partial H}{\partial t} = \frac{1}{r}\frac{\partial}{\partial r}\left(rK(h)\frac{\partial H}{\partial r}\right) \tag{7}$$

where the total hydraulic head (H) is the sum of pressure (h) and osmotic (h_π) heads and C_w (m^{-1}) is the differential water capacity $\frac{\partial H}{\partial \theta}$. Relations between K, θ and h are described by the Van Genuchten (1980) equation system (Equations 1 and 2). Analogous to Van Dam and Feddes (2000), Equation 7 can be solved using an implicit scheme of finite differences with the Picard iterative process:

$$\begin{gathered} {C_w}_i^{j+1,p-1}(H_i^{j+1,p} - H_i^{j+1,p-1}) + \theta_i^{j+1,p-1} - \theta_i^j = \frac{t^{j+1} - t^j}{r_i \Delta r_i} \times \\ \left[r_{i-1/2} K_{i-1/2}^j \frac{H_{i-1}^{j+1,p} - H_i^{j+1,p}}{r_i - r_{i-1}} - r_{i+1/2} K_{i+1/2}^j \frac{H_i^{j+1,p} - H_{i+1}^{j+1,p}}{r_{i+1} - r_i} \right] \end{gathered} \tag{8}$$

where i ($1 \leq i \leq n$) refers to the segment number, j is the time step and p the iteration level. The Picard's method is used to reduce inaccuracies in the implicit numerical solution for the h-based Equation 7 Celia et al. (1990).

The solution for Equation 8 results in prediction of pressure head in soil as a function of time and distance from the root surface. The boundary conditions considered relate the flux density entering the root to the transpiration rate for the inner segment; and considers zero flux for the outer segment:

$$K(h)\frac{\partial h}{\partial r} = q = 0\,, \qquad r = r_m \tag{9}$$

$$K(h)\frac{\partial h}{\partial r} = q_0 = \frac{T_p}{2\pi r_0 R z}\,, \qquad r = r_0 \tag{10}$$

The computer algorithm that solves the Equation 8 and applies boundary conditions 9 and 10 can be found in Appendix **??**.

The convection-dispersion equation **??** for one-dimensional axis-symmetric flow can be written as

$$r\frac{\partial(\theta C)}{\partial t} = -\frac{\partial}{\partial r}\left(rqC\right) + \frac{\partial}{\partial r}\left(rD\frac{\partial C}{\partial r}\right). \tag{11}$$

with initial condition corresponding to constant solute concentration (C_{ini}) in all segments:

$$C = C_{ini}\,, \quad t = 0,\ r = r_i,\ 1 \leq i \leq n. \tag{12}$$

Both boundary conditions are of the flux type, according to

$$-D(\theta)\frac{\partial C}{\partial r}\bigg|_{r=r_i} + qC = F\,, \quad t > 0,\ r_i = \{r_0, r_m\}\,. \tag{13}$$

From the assumed geometry (Figure 2) it follows that the boundary condition at the outer segment corresponds to zero solute flux (q_s):

$$F = 0\,, \qquad r = r_m. \tag{14}$$

The rate of solute uptake by plant roots can be described by the MM equation, as seen in Chapter **??**. The uptake shape function $\alpha(C)$ can be supposed to follow the concentration dependent MM kinetics, and considering k equal to I_m leads to:

$$\alpha(C) = \frac{C}{K_m + C} \Rightarrow F = \frac{C}{K_m + C}\, I_m \tag{15}$$

where I_m is the maximum uptake rate, C is the solute concentration in soil solution and K_m the Michaelis-Menten constant. I_m can be found experimentally and K_m is to be calibrated as the concentration at which I_m assumes half of its value, being interpreted as the affinity of the plant for the solute.

The boundary condition for solute transport at the root surface (r_0) represents the concentration dependent solute uptake, described by the MM equation 15, with the following assumptions:

- Solute uptake by mass flow of water is only controlled by the transpiration flow, a convective flow that is considered to be passive;
- Plant regulated active uptake corresponds to diffusion;
- Plant demand is equal to the I_m parameter from the MM equation;
- At a soil solution concentration value C_{lim}, the solute flux limits the uptake.

We assume that the plant demand for solute is constant in time. The uptake, however, can be higher or lower than the demand, depending on the concentration in the soil solution at the root surface (Figure 3). If the concentration is bellow a certain limiting value (C_{lim}), the uptake is limited by the solute flux, *i.e.* solute flux can not attend plant demand even with potential values of active uptake. Additionally, solute uptake by mass flow of water can be higher than the plant demand in situations of high transpiration rate and/or for high soil water content. In these cases, we assume that active uptake is zero and all uptake occurs by the passive process. A concentration C_2 (mol) for this situation is calculated. When the concentration is between C_{lim} and C_2, the uptake is equal to the plant demand as a result of the sum of active and passive contributions to the uptake. Assumption 1 states that passive uptake is not controlled by any physiological plant mechanisms and, in order to optimize the use of metabolic energy, active uptake is regulated in such way that it works as a complementary mechanism of extraction to achieve plant demand (Assumption 2). This results in a lower active uptake contribution than that of its potential value. However, the effect of the solute concentration inside the plant on solute uptake and plant demand is not considered in the model. Consequently, a scenario for which the demand is reduced due to an excess of solute concentration in the plant is not considered. This might, in certain situations, lead to an overestimated prediction of uptake.

A piecewise non-linear uptake function that considers these explicit boundary conditions was formulated as:

$$F = \begin{cases} \dfrac{I_m C_0}{K_m + C_0} + q_0 C_0, & \text{if } C_0 < C_{lim} \quad (16) \\ I_m, & \text{if } C_{lim} \leq C_0 \leq C_2 \quad (17) \\ q_0 C_0, & \text{if } C_0 > C_2 \quad (18) \end{cases}$$

with C_{lim} determined by the positive root of

$$C_{lim} = -\frac{K_m \pm \left({K_m}^2 + 4 I_m K_m / q_0\right)^{1/2}}{2}, \tag{19}$$

and C_2 by

$$C_2 = \frac{I_m}{q_0}. \tag{20}$$

The non-linear part of the uptake function resides in Equation 16. As implicit numerical implementations of non-linear functions may result in solutions with stability issues, a linearization of Equation 16 was made, resulting in:

$$F = (\alpha + q_0)\, C_0, \quad \text{if } C_0 < C_{lim} \tag{21}$$

where α (m s^{-1}) and q_0 (m s^{-1}) are the active and passive contributions for the solute uptake slope ($\alpha + q_0$). This linearization is very similar to the one proposed by Tinker and Nye (2000), but does not consider the solute concentration inside the plant. The derivation of Equations 19 to 21 is shown in Appendix **??**.

Finally, the boundary condition at the inner segment refers to the concentration dependent solute flux at the root surface (F, mol m^{-2} d^{-1}) in agreement to Equation and 21 for the non-linear and linear case, respectively. The uptake of each root equals $-F/R$ (mol d^{-1}, the negative sign indicating solute depletion), thus, the condition at the root surface is described by:

$$-D(\theta)\frac{\partial C}{\partial r} + q_0 C_0 = q_{s_0} = -\frac{F}{2\pi r_0 R z}\,, \qquad r = r_0 \tag{22}$$

Numerical implementation

TELL THAT THERE IS ALSO A LINEAR SOLUTION BUT IT WONT BE SHOWN IN THE PAPER. ALSO, THAT IT WONT BE SHOWN THE SOLUTIONS FOR THE COMPARED MODELS. CITE THE THESIS.

In the numerical solution, the combined water and solute movement is simulated iteratively. In a first step, the water movement towards the root is simulated, assuming salt concentrations from the previous time step. In a second step, the salt contents per segment are updated and new values for the osmotic head in all segments are calculated. The first step is then repeated with updated values for the osmotic heads. This process is repeated until the pressure head values and osmotic head values between iterations converge. Flowcharts containing the algorithm structure are shown in the Appendix **??**.

The implicit numerical discretization of Equation 11 yields:

$$\theta_i^{j+1} C_i^{j+1} - \theta_i^j C_i^j = \frac{\Delta t}{2 r_i \Delta r_i} \times \left\{ \frac{r_{i-1/2}}{r_i - r_{i-1}} \left[q_{i-1/2} (C_{i-1}^{j+1} \Delta r_i + C_i^{j+1} \Delta r_{i-1}) - 2 D_{i-1/2}^{j+1} (C_i^{j+1} - C_{i-1}^{j+1}) \right] - \frac{r_{i+1/2}}{r_{i+1} - r_i} \left[q_{i+1/2} (C_i^{j+1} \Delta r_{i+1} + C_{i+1}^{j+1} \Delta r_i) - 2 D_{i+1/2}^{j+1} (C_{i+1}^{j+1} - C_i^{j+1}) \right] \right\} \tag{23}$$

Applying equation 23 to each segment, the concentrations for the next time step C_i^{j+1} (mol m^{-3}) are obtained by solving the following tridiagonal matrix:

$$\begin{bmatrix} b_1 & c_1 & & & & \\ a_2 & b_2 & c_2 & & & \\ & a_3 & b_3 & c_3 & & \\ & & \ddots & \ddots & \ddots & \\ & & & a_{n-1} & b_{n-1} & c_{n-1} \\ & & & & a_n & b_n \end{bmatrix} \begin{bmatrix} C_1^{j+1} \\ C_2^{j+1} \\ C_3^{j+1} \\ \vdots \\ C_{n-1}^{j+1} \\ C_n^{j+1} \end{bmatrix} = \begin{bmatrix} f_1 \\ f_2 \\ f_3 \\ \vdots \\ f_{n-1} \\ f_n \end{bmatrix} \tag{24}$$

with f_i(mol m^{-2}) defined as

$$f_i = r_i \theta_i^j C_i^j \tag{25}$$

and a_i (m), b_i (m) and c_i (m) defined for the respective segments as described in the following.

1. The intermediate nodes **($i = 2$ to $i = n - 1$)**

   Rearrangement of Equation 23 to 24 results in the coefficients:

$$a_i = -\frac{r_{i-1/2} (2 D_{i-1/2}^{j+1} + q_{i-1/2} \Delta r_i) \Delta t}{2 (r_i - r_{i-1}) \Delta r_i} \tag{26}$$

$$b_i = r_i \theta_i^{j+1} + \frac{\Delta t}{2 \Delta r_i} \left[\begin{array}{l} \frac{r_{i-1/2}}{(r_i - r_{i-1})} (2 D_{i-1/2}^{j+1} - q_{i-1/2} \Delta r_{i-1}) + \\ \frac{r_{i+1/2}}{(r_{i+1} - r_i)} (2 D_{i+1/2}^{j+1} + q_{i+1/2} \Delta r_{i+1}) \end{array} \right] \tag{27}$$

$$c_i = -\frac{r_{i+1/2} \Delta t}{2 \Delta r_i (r_{i+1} - r_i)} (2 D_{i+1/2}^{j+1} - q_{i+1/2} \Delta r_i) \tag{28}$$

2. The outer boundary **($i = n$)**

   Applying boundary condition of zero solute flux, the third and fourth terms from the right hand side of Equation 23 are equal to zero. Thus, the solute balance for this segment is written as:

$$\theta_n^{j+1}C_n^{j+1} - \theta_n^j C_n^j = \frac{\Delta t}{2r_n\Delta r_n}\times \left\{ \frac{r_{n-1/2}}{r_n - r_{n-1}} \left[\begin{array}{l} q_{n-1/2}(C_{n-1}^{j+1}\Delta r_n + C_n^{j+1}\Delta r_{n-1}) - \\ 2D_{n-1/2}^{j+1}(C_n^{j+1} - C_{n-1}^{j+1}) \end{array} \right] \right\} \tag{29}$$

Rearrangement of Equation 29 to 24 results in the coefficients:

$$a_n = -\frac{r_{n-1/2}(2D_{n-1/2}^{j+1} + q_{n-1/2}\Delta r_n)\Delta t}{2(r_n - r_{n-1})\Delta r_n} \tag{30}$$

$$b_n = r_n\theta_n^{j+1} + \frac{\Delta t}{2\Delta r_n}\left[\frac{r_{n-1/2}}{r_n - r_{n-1}}(2D_{n-1/2}^{j+1} + q_{n-1/2}\Delta r_{n-1})\right] \tag{31}$$

3. The inner boundary $\boldsymbol{(i = 1)}$

(a) For $\boldsymbol{C < C_{lim}}$

Applying boundary conditions of non-linear concentration dependent solute flux, the first and second term of the right-hand side of Equation 23 become $-\left(\frac{I_m}{2\pi r_0 Rz(K_m + C_1^{j+1})} + q_0\right)C_1^{j+1}\Delta r_1$:

$$\theta_1^{j+1}C_1^{j+1} - \theta_1^j C_1^j = \frac{\Delta t}{2r_1\Delta r_1}\times \left\{ \begin{array}{l} \frac{r_{1-1/2}}{r_1 - r_0}\left[-\left(\frac{I_m}{2\pi r_0 Rz(K_m + C_1^{j+1})} + q_0\right)\right] C_1^{j+1}\Delta r_1 - \\ \frac{r_{1+1/2}}{r_2 - r_1}\left[\begin{array}{l} q_{1+1/2}(C_1^{j+1}\Delta r_2 + C_2^{j+1}\Delta r_1) - \\ 2D_{1+1/2}^{j+1}(C_2^{j+1} - C_1^{j+1}) \end{array} \right] \end{array} \right\} \tag{32}$$

Rearrangement of Equation 32 to 24 results in the following coefficients:

$$b_1 = r_1\theta_1^{j+1} + \frac{\Delta t}{2\Delta r_1}\left[\begin{array}{l} \frac{r_{1+1/2}}{(r_2 - r_1)}(2D_{1+1/2}^{j+1} + q_{i+1/2}\Delta r_2) + \\ \frac{r_{1-1/2}}{r_1 - r_0}\left(\frac{I_m}{2\pi r_0 Rz(K_m + C_1^{j+1})} + q_0\right)\Delta r_1 \end{array} \right] \tag{33}$$

$$c_1 = -\frac{r_{1+1/2}\Delta t}{2\Delta r_1(r_2 - r_1)}(2D_{1+1/2}^{j+1} - q_{1+1/2}\Delta r_1) \tag{34}$$

(b) For $\boldsymbol{C_{lim} < C < C_2}$

The constant uptake solution is based on the model proposed by De Willigen and Van Noordwijk (1994). The numerical discretization takes into consideration Equation 23, whereas the intermediate nodes are analogous to Equations 26 to 28. The boundary condition at the root surface (Equation 22) corresponds to constant solute flux:

$$q_{s0} = -\frac{I_m}{2\pi r_0 Rz}. \tag{35}$$

Applying boundary conditions of constant solute flux, the first and second term of the right-hand side of Equation 23 become $-\frac{I_m}{2\pi r_0 Rz}\Delta r_1$ for $C > 0$:

$$\theta_1^{j+1}C_1^{j+1} - \theta_1^j C_1^j = \frac{\Delta t}{2r_1\Delta r_1}\times \left\{ \begin{array}{l} \frac{r_{1-1/2}}{r_1 - r_0}\left(-\frac{I_m}{2\pi r_0 Rz}\right)\Delta r_1 - \\ \frac{r_{1+1/2}}{r_2 - r_1}\left[\begin{array}{l} q_{1+1/2}(C_1^{j+1}\Delta r_2 + C_2^{j+1}\Delta r_1) - \\ 2D_{1+1/2}^{j+1}(C_2^{j+1} - C_1^{j+1}) \end{array} \right] \end{array} \right\} \tag{36}$$

When $C = 0$ the solute flux is set to zero and equation 36 reduces to Equation 41. Introduction of Equation 36 in the tridiagonal matrix 24 results in the following coefficients:

$$b_1 = r_1\theta_1^{j+1} + \frac{\Delta t}{2\Delta r_1}\left[\frac{r_{1+1/2}}{(r_2 - r_1)}(2D_{1+1/2}^{j+1} + q_{1+1/2}\Delta r_2)\right] \tag{37}$$

$$c_1 = -\frac{r_{1+1/2}\Delta t}{2\Delta r_1(r_2 - r_1)}(2D_{1+1/2}^{j+1} - q_{1+1/2}\Delta r_1) \tag{38}$$

And the f coefficient changes to:

$$f_1 = r_1\theta_1^j C_1^j - \frac{r_{1-1/2}}{r_1 - r_0} I_m \frac{\Delta t}{4\pi r_0 Rz} \tag{39}$$

(c) For $\boldsymbol{C = 0}$

When $C = 0$ the solute flux is set to zero and the equation is equal to Equation 41 (zero uptake). The zero uptake solution is based on the model proposed by De Jong van Lier et al. (2009). The numerical discretization is according to Equation 23 and the intermediate nodes are analogous to Equations 26 to 28. The only difference is the boundary at the root surface (Equation 22), which is of zero solute flux:

$$q_{s0} = 0 \tag{40}$$

Applying boundary condition of zero solute flux, the first and second term of the right-hand side of Equation 23 are equal to zero:

$$\begin{aligned}\theta_1^{j+1}C_1^{j+1} - \theta_1^j C_1^j = \frac{\Delta t}{2r_1\Delta r_1}\times \\ \left\{\frac{r_{1+1/2}}{r_2 - r_1}\left[\begin{array}{l} -q_{1+1/2}(C_1^{j+1}\Delta r_2 + C_2^{j+1}\Delta r_1) + \\ 2D_{1+1/2}^{j+1}(C_2^{j+1} - C_1^{j+1}) \end{array}\right]\right\}\end{aligned} \tag{41}$$

Introduction of Equation 41 in the tridiagonal matrix 24 results in the following coefficients:

$$b_1 = r_1\theta_1^{j+1} + \frac{\Delta t}{2\Delta r_1}\left[\frac{r_{1+1/2}}{(r_2 - r_1)}(2D_{1+1/2}^{j+1} + q_{1+1/2}\Delta r_2)\right] \tag{42}$$

$$c_1 = -\frac{r_{1+1/2}\Delta t}{2\Delta r_1(r_2 - r_1)}(2D_{1+1/2}^{j+1} - q_{1+1/2}\Delta r_1) \tag{43}$$

Simulation Scenarios

The simulations were performed using the hydraulic parameters from the Dutch Staring series Wösten et al. (2001) for three different soils types, as listed in Table 1. The general system parameters for the different scenarios are listed in Table 2 and values for the Michaelis-Menten (MM) parameters in Table 4. Values of root length density, initial solute concentration, relative transpiration, soil type, and ion species were chosen at several values, composing eight distinct scenarios as listed in Table **??**. Scenario 1 was considered as default, the other scenarios derive from scenario 1 by changing only one input parameter. In this way, the effect of variation in soil hydraulic properties is exemplified by scenarios 1, 6 and 7; root length density by scenarios 1, 4 and 5; initial solute concentration by scenarios 1 and 3; and potential transpiration by scenarios 1 and 2.

The default values of Δr_{min}, Δr_{max} and S in Equation 6 were 10^{-5} m, 5 10^{-4} m and 0.5, resulting in 22, 68 and 213 segments for the high, medium and low root density simulations, respectively. To guarantee complete convergence for the non-linear model, a time step of 0.01 s was used when $C_0 < C_{lim}$. Parameters h_{ini} and C_{ini} were chosen such that the plant is in a no stress condition ($T_r = 1$). All simulation scenarios ended when $T_r \leq 0.001$, at that point considering water uptake to be negligible.

Table 2: System parameters used in simulations scenarios

Description	Symbol	Scenario description	Value	Unit
Root radius	r_0		0.5	mm
Root depth	z		20	cm
Limiting root potential	h_{lim}		-150	m
Root density	R	Low root density Medium root density High root densit	0.01 0.1 1	cm cm^{-3}
Half distance between roots	r_m	Low root density Medium root density High root densit	56.5 17.8 5.65	mm
Potential transpiration rate	T_p	Low High	3 6	mm d^{-1}
Initial solute concentration in bulk soil	C_{ini}	Low High	1 10	mol m^{-3}
Initial pressure head	h_{ini}		-1	m
Diffusion coefficient in water	$D_{m,w}$		$1.98 \cdot 10^{-9}$	m^2 s^{-1}
Dispersivity	τ		0.0005	m
Soil type		Sand Clay Loam	Table 1	

Table 3: Michaelis-Menten parameters for some solutes

Solute	I_m mol m^{-2} s^{-1}	K_m mol m^{-3}
NO_3^-	10^{-5}	0.05
K^+	$2 \cdot 10^{-6}$	0.025
$H_2PO_4^-$	10^{-6}	0.005
Cd^{2+}	10^{-6}	1

Table 4: Simulation scenarios

Scenario	R	C_{ini}	T_p	Soil	Ion
1	M	H	H	Loam	K^+
2	M	H	L	Loam	K^+
3	M	L	H	Loam	K^+
4	H	H	H	Loam	K^+
5	L	H	H	Loam	K^+
6	M	H	H	Sand	K^+
7	M	H	H	Clay	K^+
8	M	H	H	Loam	NO_3^-

Analysis of linear and non-linear approaches

To analyze the differences between the two proposed models (linear and non-linear solutions), the relative differences in the predicted concentrations (δ_C) and accumulated uptake (δ_{Ac}), for both models, were calculated as follows:

$$\delta_C = \frac{\sum_{x=1}^{x_{end}} CL_x - CNL_x}{\sum_{x=1}^{x_{end}} CL_x} \tag{44}$$

$$\delta_{Ac} = \frac{\sum_{t=1}^{t_{end}} AcL_t - AcNL_t}{\sum_{t=1}^{t_{end}} AcL_t} \tag{45}$$

$$\tag{46}$$

where CL_x and CNL_x, are the solute concentration in soil water, and AcL_t and $AcNL_t$ the accumulated uptake, for LU and NLU, respectively. x can be the time (t) or the distance from the axial center (r). The relative difference between three outputs was computed: two relative to time – concentration at the root surface $C_0(t)$ and accumulated solute uptake $Ac(t)$ – and one relative to radial distance – concentration $C(r)$.

NLU solution uses the non-linear MM equation and, due to an additional iterative process in the numerical implementation, more time is needed to compute the results when compared with the linear solution LU. It is also susceptible to numerical stability issues, depending on selected time and space steps. On the other hand, LU is a simplified version of the MM equation in a way that the solute uptake rate for $C_0 < C_{lim}$ is always smaller than that of the original non-linear equation. It has no stability problems and needs less computational time because it is less sensitive to space and time steps. In a first analysis, the objective was to check if the difference in the results generated by the linearization of the MM equation is sufficiently large to be properly analyzed. To do so, four different scenarios were chosen (scenarios 1 to 4 as listed in Table **??**).

Sensitivity analysis

The relative partial sensitivity η de Jong van Lier et al. (2015) of model predictions Y as a function of the respective parameter value P was calculated as

$$\eta = \frac{dY/Y}{dP/P} \tag{47}$$

where P is the default value of the parameter, dP is the in(de)crement applied to P, Y is the output of a selected predicted variable and dY is the variation over Y when applied the new parameter value $P \pm dP$.

To determine the sensitivity of the model to an input parameter, the magnitude of its derivative in respect of the model result is calculated. If this derivative is close to zero, the model has a low sensitivity to the respective parameter. The higher the derivative, the higher is the sensitivity and, therefore, the higher is the precision required when determining that parameter. By making a relative analysis like in Equation 47, the sensitivity for distinct parameters can be compared.

To determine the sensitivity, a dP/P of 0.01 (1%) was used for the following selected parameters: a) MM parameters I_m, K_m; and b) soil hydraulic parameters α, n, λ, K_s, θ_r and θ_s. The analyzed predicted variables (Y) were: time to completion of simulation t_{end}, osmotic head at completion of simulation h_π, pressure head at completion of simulation h, average osmotic head in the soil profile at completion of simulation $\overline{h_\pi}$, average pressure head in soil profile at completion of simulation $\overline{h}$ and accumulated uptake at completion of simulation Ac.

Acknowledgements

The first author would like to thank to the National Counsel of Technological and Scientific Development (CNPq) for the scholarship granted during his PhD, to Coordination for the Improvement of Higher Education Personnel (CAPES) for the scholarship granted during the sandwich internship at the Wageningen University, Netherlands, and also to Peter de Willigen for his valuable contributions in the formulation of the mathematical framework of this study.

References

S A Barber. Influence of the plant root on ion movement in soil. In E W Carson, editor, *The plant root and its enviroment*, pages 525–564. Procedures in plant roots and their enviroment, Charlottesville, 1974.

S A Barber and J H Cushman. Nitrogen uptake model for agronomic crops. In I K Iskander, editor, *Modelling wastewater renovation for land treatment*, pages 382–489. Wiley Interscience, New York, 1981.

Stanley A Barber. A diffusion and mass-flow concept of soil nutrient availability. *Soil Science*, 93(1): 39–49, 1962.

Stanley A Barber. *Soil nutrient bioavailability: a mechanistic approach.* John Wiley & Sons, New York, 2 edition, 1995.

P B Barraclough and R A Leigh. The growth and activity of winter wheat roots in the field: the effect of sowing date and soil type on root growth of high-yielding crops. *The Journal of Agricultural Science*, 103(01):59–74, 1984.

AC Borstlap. The use of model-fitting in the interpretation of dual uptake isotherms. *Plant, Cell & Environment*, 6(5):407–416, 1983.

Martin R Broadley, Philip J White, John P Hammond, Ivan Zelko, and Alexander Lux. Zinc in plants. *New Phytologist*, 173(4):677–702, 2007.

Michael A Celia, Efthimios T Bouloutas, and Rebecca L Zarba. A general mass-conservative numerical solution for the unsaturated flow equation. *Water resources research*, 26(7):1483–1496, 1990.

John H. Cushman. An analytical solution to solute transport near root surfaces for low initial concentration: I. equations development. *Soil Science Society of America Journal*, 43(6):1087–1090, 1979.

Quirijn De Jong van Lier, Klaas Metselaar, and Jos C. Van Dam. Root water extraction and limiting soil hydraulic conditions estimated by numerical simulation. *Vadose Zone Journal*, 5(4):1264–1277, 2006.

Quirijn De Jong van Lier, Jos C. Van Dam, and Klaas Metselaar. Root water extraction under combined water and osmotic stress. *Soil Science Society of America Journal*, 73(3):862–875, 2009.

Quirijn de Jong van Lier, Ole Wendroth, and Jos C. van Dam. Prediction of winter wheat yield with the swap model using pedotransfer functions: An evaluation of sensitivity, parameterization and prediction accuracy. *Agricultural Water Management*, 154(1):29–42, 2015.

Peter De Willigen. Mathematical analysis of diffusion and mass flow of solutes to a root assuming constant uptake. Technical report, Instituut voor Bodemvruchtbaarheid, Haren, 1981. Techinical Report.

Peter De Willigen and Meine Van Noordwijk. Mass flow and diffusion of nutrients to a root with constant or zero-sink uptake i. constant uptake. *Soil science*, 157(3):162–170, 1994.

Emanuel Epstein. Spaces, barriers, and ion carriers: ion absorption by plants. *American Journal of Botany*, 47(5):393–399, 1960.

Emanuel Epstein. *Mineral nutrition of plants: principles and perspectives.* Science Reviews 2000, London, 1972.

Reinder A Feddes, Piotr J Kowalik, and Henryk Zaradny. *Simulation of field water use and crop yield.* Centre for Agricultural Publishing and Documentation, Wageningen, 1978.

Maurice Fried and Raymond E Shapiro. Soil-plant relationships in ion uptake. *Annual Review of Plant Physiology*, 12(1):91–112, 1961.

W R Gardner. Dynamic aspects of soil-water availability to plants. *Annual review of plant physiology*, 16(1):323–342, 1965.

Mehdi Homaee. *Root water uptake under non-uniform transient salinity and water stress*. PhD thesis, Wageningen University, 1999.

J M Kelly and S A Barber. Magnesium uptake kinetics in loblolly pine seedlings. *Plant and soil*, 134(2): 227–232, 1991.

Leon V Kochian and William J Lucas. Potassium transport in corn roots i. resolution of kinetics into a saturable and linear component. *Plant Physiology*, 70(6):1723–1731, 1982.

Hans Lambers, F Stuart Chapin III, and Thijs L Pons. *Plant water relations*, chapter Chapter 3, pages 163–223. Springer, New York, 2008.

K. Y. Li, R. De Jong, M. T. Coe, and N. Ramankutty. Root-water-uptake based upon a new water stress reduction and an asymptotic root distribution function. *Earth Interactions*, 10(14):1–22, 2006.

Alexander Lux, Michal Martinka, Marek Vaculík, and Philip J White. Root responses to cadmium in the rhizosphere: a review. *Journal of Experimental Botany*, 62(1):21–37, 2011.

P H Nye and F H C Marriott. A theoretical study of the distribution of substances around roots resulting from simultaneous diffusion and mass flow. *Plant and Soil*, 30(3):459–472, 1969.

Peter Hague Nye and Philip Bernard Tinker. *Solute movement in the soil-root system*. University of California Press, Berkeley, 1977.

Tiina Roose, A C Fowler, and P R Darrah. A mathematical model of plant nutrient uptake. *Journal of mathematical biology*, 42(4):347–360, 2001.

Upkar Singh Sadana, Parmodh Sharma, Nelson Castañeda Ortiz, Debasmita Samal, and Norbert Claassen. Manganese uptake and mn efficiency of wheat cultivars are related to mn-uptake kinetics and root growth. *Journal of Plant Nutrition and Soil Science*, 168(4):581–589, 2005.

Natalie Schröder, Mathieu Javaux, Jan Vanderborght, Bernhard Steffen, and Harry Vereecken. Effect of root water and solute uptake on apparent soil dispersivity: A simulation study. *Vadose Zone Journal*, 11(3):1–14, 2012.

Björn Seeling and Norbert Claassen. A method for determining michaelis-menten kinetic parameters of nutrient uptake for plants growing in soil. *Zeitschrift für Pflanzenernährung und Bodenkunde*, 153(5): 301–303, 1990.

Jianchu Shi, Alon Ben-Gal, Uri Yermiyahu, Lichun Wang, and Qiang Zuo. Characterizing root nitrogen uptake of wheat to simulate soil nitrogen dynamics. *Plant and soil*, 363(1-2):139–155, 2013.

M Yaeesh Siddiqi, Anthony DM Glass, Thomas J Ruth, and Thomas W Rufty. Studies of the uptake of nitrate in barley i. kinetics of 13no3-influx. *Plant Physiology*, 93(4):1426–1432, 1990.

J Šimùnek, M Šejna, and M Th Van Genuchten. The hydrus software package for simulating the two-and three-dimensional movement of water, heat, and multiple solutes in variably-saturated media. *Technical manual*, 1(1):241, 2006.

Jiří Šimunek and Jan W Hopmans. Modeling compensated root water and nutrient uptake. *Ecological modelling*, 220(4):505–521, 2009.

F Somma, J W Hopmans, and V Clausnitzer. Transient three-dimensional modeling of soil water and solute transport with simultaneous root growth, root water and nutrient uptake. *Plant and Soil*, 202 (2):281–293, 1998.

P.B. Tinker and P.H. Nye. *Solute Movement in the Rhizosphere*. Topics in sustainable agronomy. Oxford University Press, 2000.

Augusto J Vallejo, Maria Luisa Peralta, and GUILLERMO E SANTA-MARIA. Expression of potassium-transporter coding genes, and kinetics of rubidium uptake, along a longitudinal root axis. *Plant, Cell & Environment*, 28(7):850–862, 2005.

Jos C Van Dam and Reinder A Feddes. Numerical simulation of infiltration, evaporation and shallow groundwater levels with the richards equation. *Journal of Hydrology*, 233(1):72–85, 2000.

Jos C Van Dam, Piet Groenendijk, Rob F A Hendriks, and Joop G Kroes. Advances of modeling water flow in variably saturated soils with swap. *Vadose Zone Journal*, 7(2):640–653, 2008.

M Th Van Genuchten. A closed-form equation for predicting the hydraulic conductivity of unsaturated soils. *Soil science society of America journal*, 44(5):892–898, 1980.

Miao Yuan Wang, M Yaeesh Siddiqi, Thomas J Ruth, and Anthony DM Glass. Ammonium uptake by rice roots (ii. kinetics of 13nh4+ influx across the plasmalemma). *Plant physiology*, 103(4):1259–1267, 1993.

J H M Wösten, G J Veerman, W J M De Groot, and J Stolte. Waterretentie-en doorlatendheidskarakteristieken van boven-en ondergronden in nederland: de staringsreeks. 2001.

Figures

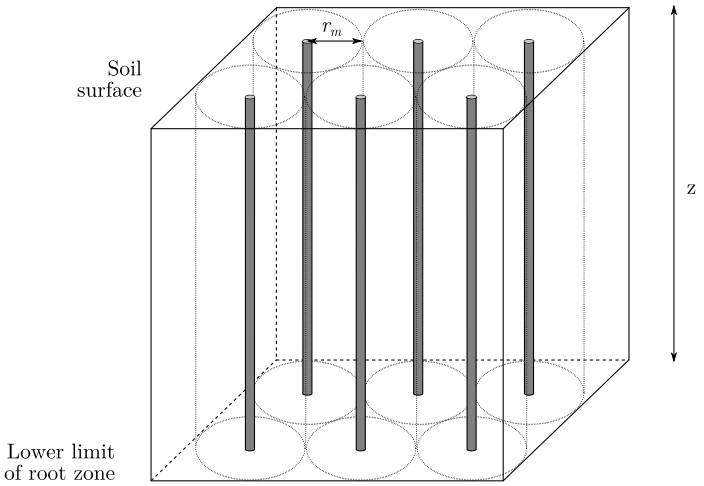

Figure 1: Schematic representation of the spatial distribution of roots in the root zone

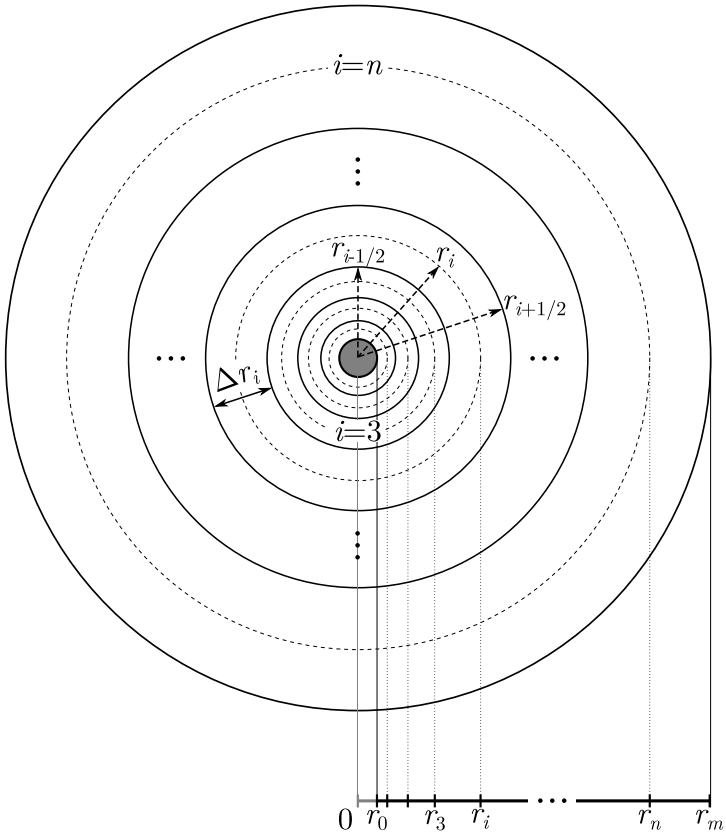

Figure 2: Schematic representation of the discretized domain considered in the model. Δr is the variable segment size, increasing with the distance from the root surface (r_0) to the half-distance between roots (r_m), and n is the number of segments

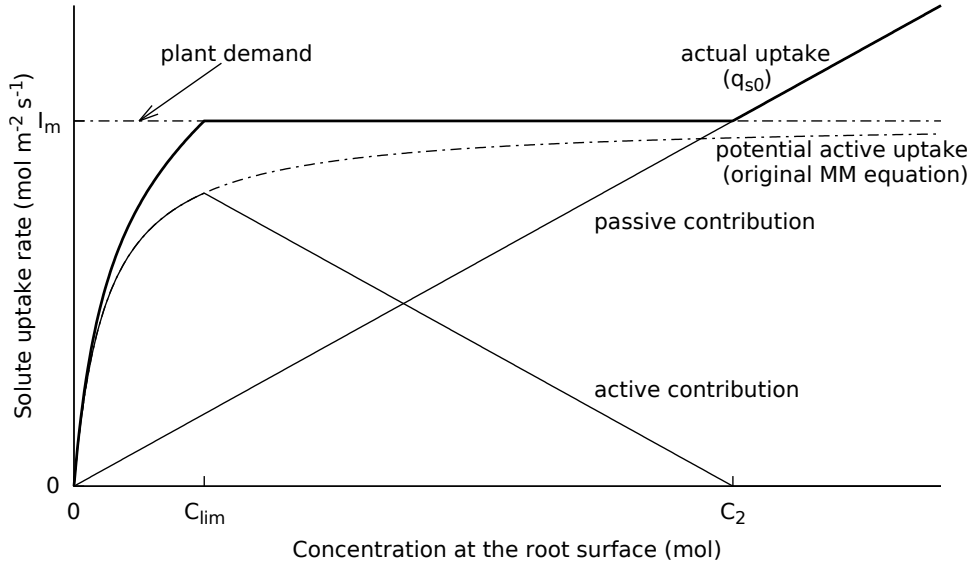

Figure 3: Solute uptake piecewise equation from MM equation 15 with boundary conditions. The bold line represents the actual uptake, thin lines represent active and passive contributions to the actual uptake, and dotted lines represent the plant demand and the potential active uptake